

Inertia-gravity-wave generation by balanced motion: revisiting the Lorenz–Krishnamurthy model

J. Vanneste*

School of Mathematics,

University of Edinburgh,

Edinburgh, UK

Revised version, June 2003

*Corresponding author address: J. Vanneste, School of Mathematics, University of Edinburgh, King's Buildings, Mayfield Road, Edinburgh EH9 3JZ, United Kingdom. Email: J.Vanneste@ed.ac.uk

The spontaneous generation of inertia-gravity waves by balanced motion at low Rossby number is examined using Lorenz's five-component model. The mostly numerical analysis by Lorenz & Krishnamurthy of a particular (homoclinic) balanced solution is complemented here by an asymptotic analysis. An exponential-asymptotic technique provides an estimate for the amplitude of the fast inertia-gravity oscillations which are generated spontaneously, through what is shown to be a Stokes phenomenon. This estimate is given by $2\pi\kappa\epsilon^{-2}\exp[-\pi/(2\epsilon)]$, where $\epsilon \ll 1$ is proportional to the Rossby number and the prefactor κ is determined from recurrence relations. The nonlinear dependence of κ on the $O(1)$ rotational Froude number indicates that the feedback of the inertia-gravity waves on the balanced motion directly affects their amplitude.

Numerical experiments confirm the analytic results. Optimally truncated slaving relations are used to separate the exponentially small inertia-gravity oscillations from the (much larger) slow contribution to the dependent variables. This makes it possible to examine the switching-on of the oscillations in detail; it is shown to be described by an error function of $t/\epsilon^{1/2}$ as predicted theoretically. The results derived for the homoclinic solution of Lorenz & Krishnamurthy are extended to more general, periodic, solutions.

1 Introduction

Initialisation, slow manifold, balanced dynamics and other related concepts can usefully be understood by studying finite-dimensional, low-order models. This approach was pioneered by Lorenz who introduced, in particular, a five-component truncation of the shallow-water equations (Lorenz 1986) which has become a central tool in the investigation of these concepts. The model is often referred to as the Lorenz–Krishnamurthy model, after the subsequent work in which a forced-dissipative version was introduced to examine the spontaneous generation of inertia-gravity waves by balanced motion (Lorenz & Krishnamurthy 1987). Since then, the Lorenz–Krishnamurthy model, either in conservative or forced-dissipative versions, has been the subject of many papers (Jacobs 1991, Lorenz 1992, Boyd 1994, Fowler & Kember 1996, Camassa 1995, Boyd 1995, Bokhove & Shepherd 1996, Camassa & Tin 1996, to give a long, yet non-exhaustive, list). The reason for this appeal is that the model is arguably the simplest in which the interactions between slow vortical modes (represented by a triad of Rossby waves) and fast inertia-gravity modes (represented by a pair of inertia-gravity waves) are described in a realistic manner.

Lorenz & Krishnamurthy (1987) examined a particular solution of their model in the small-Rossby-number limit to demonstrate that a solution that is initially perfectly balanced inevitably develops fast inertia-gravity oscillations in the course of time. This has two major implications: (i) it establishes the non-existence of an exactly invariant slow manifold for the model (see also Lorenz (1986) and Bokhove & Shepherd (1996) for further discussion and the definition of a slowest “manifold”); and (ii) it exhibits a physical mechanism for the spontaneous generation of inertia-gravity waves.

It is of interest, especially in view of the practical implications of (ii), to estimate

the amplitude of the inertia-gravity waves that are generated. Lorenz & Krishnamurthy (1987) used numerical solutions to show that this amplitude is exponentially small; that is, it is proportional to $\exp(-\alpha/\epsilon)$, where $\epsilon \ll 1$ is the relevant small parameter and $\alpha > 0$ a constant. In terms of the rotational Froude number b and Rossby number R , ϵ is defined by

$$\epsilon = \frac{bR}{\sqrt{1+b^2}}, \quad (1.1)$$

and it can be recognized as the ratio of the nonlinear frequency Rf , with f the Coriolis parameter, to the inertia-gravity-wave frequency $f\sqrt{1+1/b^2}$ (Bokhove & Shepherd 1996). Lorenz & Krishnamurthy (1987) supported their numerical results by an analytical estimate which assumes that $b \ll 1$ in addition to (and prior to) $\epsilon \ll 1$. The aim of the present paper is the derivation of a more general analytic estimate, valid in the regime where $b = O(1)$, $R \ll 1$ and hence $\epsilon = O(R) \ll 1$. This is the usual low-Rossby-number quasi-geostrophic regime, the regime relevant to Lorenz & Krishnamurthy (1987)'s numerical calculations.

To derive this estimate and capture the exponentially small gravity-wave amplitude, we use the techniques of exponential asymptotics, or asymptotics beyond all orders (see, e.g., Segur, Tanveer & Levine (1991)). The relevance of these techniques to the problem at hand has been pointed out in the past (Boyd 1995, Fowler & Kember 1996) but their application seems to be new. Vanneste & Yavneh (2003) use exponential asymptotics to estimate the amplitude of the inertia-gravity waves that appear spontaneously in a family of exact, sheared-disturbance, solutions to the three-dimensional Boussinesq equations which are described by a (non-autonomous) linear ordinary differential equation. The present paper treats the Lorenz–Krishnamurthy model in a similar manner. There are, however, important differences mostly because the Lorenz–Krishnamurthy model is nonlinear. As a result, the connection problem which underlies the exponential-asymptotic analysis cannot be solved in closed form,

in contrast to that in Vanneste & Yavneh (2003). The amount of numerical calculation that is required is nevertheless modest: the use of a Borel-summation technique reduces the problem to the determination of a single function of b that is obtained from a (nonlinear) recursion.

The generation of exponentially small inertia-gravity waves from balanced motion occurs through a Stokes phenomenon (e.g., Olver (1974) or Ablowitz & Fokas (1997)). It corresponds to the switching-on of a subdominant term (associated with the waves) when the real-valued time t crosses a Stokes line which emanates from singularities of the balanced motion in the complex t -plane. Physically, this means that the waves appear quite suddenly near a fixed time which is easy to identify. The theory of the Stokes phenomenon (Berry 1989) provides a detailed description of the manner in which the subdominant term is switched on. We confirm the relevance of this description to the inertia-gravity-wave problem by showing that the wave amplitude estimated from numerical solutions behaves as an error-function of $t/\epsilon^{1/2}$, in agreement with the theoretical prediction of Berry (1989).

It should be noted that our analysis is local in time in that it accurately describes the dynamics only for a finite, $O(1)$, time after the inertia-gravity-wave generation. While the inertia-gravity waves leave the balanced motion essentially unaffected on such time scales, they have a systematic effect on longer times scales ($O(\epsilon^{-1})$ or larger). This systematic effect is, of course, crucial when global issues, such as the existence of invariant (but not slow) manifolds, are addressed. The (formal) asymptotic techniques used in this paper are not appropriate to study such issues. (See, e.g., Lorenz (1992), Camassa (1995), Bokhove & Shepherd (1996) and Camassa & Tin (1996) for some global results.)

The plan of the paper is as follows. In §2 we introduce the Lorenz–Krishnamurthy model and the particular solution (homoclinic to a fixed point when $\epsilon = 0$) under con-

sideration. The exponential-asymptotic analysis leading to an estimate for the amplitude of the inertia-gravity waves is carried out in §3. This estimate is checked against numerical results in §4. The rapidly oscillating, inertia-gravity-wave component of the numerical solutions is isolated from the much larger slow balanced component using high-order slaving (Warn, Bokhove, Shepherd & Vallis 1995, Bokhove & Shepherd 1996). This technique is sufficiently accurate to capture the switching-on of inertia-gravity waves and demonstrate its agreement with the theoretical prediction. The paper concludes with a few remarks in §5.

Most of the paper is devoted to the homoclinic balanced solution considered by Lorenz & Krishnamurthy (1987). As is well known, this solution is the limiting member of a one-parameter family of periodic solutions which can be written in terms of elliptic functions. We devote Appendix A to the derivation of an estimate for the amplitude of the inertia-gravity waves that are generated by these more general balanced solutions. This analytic estimate is confirmed numerically.

2 Model

We consider Lorenz's five-component model (Lorenz 1986) in the conservative (or inviscid) form

$$\begin{aligned}
 \dot{u} &= -vw + \epsilon bvy, \\
 \dot{v} &= uw - \epsilon buy, \\
 \dot{w} &= -uv, \\
 \epsilon \dot{x} &= -y, \\
 \epsilon \dot{y} &= x + bwv,
 \end{aligned} \tag{2.1}$$

where ϵ is related to the rotational Froude number b and Rossby number R according to (1.1). The variables have been scaled following Bokhove & Shepherd (1996), but with an additional factor ϵ for the fast variables x and y . (It may be noted that (2.1) reduces to a two-degree-of-freedom Hamiltonian system (Camassa 1995, Bokhove & Shepherd 1996), although we make no explicit use of this fact.)

An approximate balance is possible when $\epsilon \ll 1$. In this limit, (2.1) describes the interaction between a slow Rossby-wave triad (u, v, w) with $O(1)$ (nonlinear) frequency, and a fast inertia-gravity-wave pair (x, y) with (linear) frequency $1/\epsilon \gg 1$. It is, of course, on this formal frequency separation that the concept of balance rests. In this paper, we concentrate on one of the possible ways to approach the limit $\epsilon \ll 1$, namely $R \ll 1$ and $b = O(1)$. This corresponds to the standard quasi-geostrophic regime, with small Rossby and Froude numbers R and $F = Rb$ (cf. Pedlosky (1987)).

When $\epsilon = 0$, the slow variables (u, v, w) decouple from the fast ones (x, y) , and exact solutions of (2.1) are readily found. Following Lorenz & Krishnamurthy (1987), we consider mainly the homoclinic solution

$$u_0 = \operatorname{sech} t, \quad v_0 = -\tanh t, \quad w_0 = -\operatorname{sech} t, \quad x_0 = -bu_0v_0, \quad y_0 = 0, \quad (2.2)$$

which, clearly, is formally slow, devoid of inertia-gravity oscillations. More general, periodic, solutions are considered in Appendix A. (Note that there is no loss of generality in taking unit amplitudes for the hyperbolic functions in (2.2) as this can be arranged by suitably defining ϵ . Moreover, the signs of any pair in (u_0, v_0, w_0) can be changed freely; here we follow the choice of Lorenz & Krishnamurthy (1987).)

When $\epsilon \neq 0$, it is natural to seek a slow solution as a perturbation of (2.2). This is achieved formally by introducing expansions of the form

$$u_{\text{bal}} = \sum_{n=0}^N \epsilon^n u_n, \quad \dots \quad (2.3)$$

into (2.1) and solving order by order for the coefficients u_n , v_n , etc. up to some

order $n = N$. The solutions so obtained are balanced approximations, hence the subscript *bal*, which do not contain explicit fast oscillations and satisfy the following symmetries:

$$\begin{aligned} u_{\text{bal}}(-t) &= u_{\text{bal}}(t), & v_{\text{bal}}(-t) &= -v_{\text{bal}}(t), & w_{\text{bal}}(-t) &= w_{\text{bal}}(t), \\ x_{\text{bal}}(-t) &= -x_{\text{bal}}(t), & y_{\text{bal}}(-t) &= y_{\text{bal}}(t). \end{aligned} \tag{2.4}$$

That they cannot capture the dynamics of (2.1) completely, however small ϵ and however large N , emerges from two pieces of evidence. Firstly, the balanced approximations (2.3) are only asymptotic and generally diverge as $N \rightarrow \infty$ (Lorenz 1986). This can be attributed to their failure to capture exponentially small terms, expected to represent fast inertia-gravity oscillations. Secondly, such oscillations appear clearly in the numerical solutions of (2.1): as shown by Lorenz & Krishnamurthy (1987), solutions that are well balanced for $t \rightarrow -\infty$ develop exponentially small inertia-gravity for $t > 0$.

Figure 1, which is similar to Figure 5 in Lorenz & Krishnamurthy (1987), illustrates this point. It shows the evolution of the fast variable $y(t)$ for $b = 0.5$ and for three different values of ϵ . This evolution has been obtained by solving (2.1) numerically, starting with the leading-order balanced solution (2.2) at some large negative time (specifically $t = -10$). While $y(t)$ remains apparently balanced as long as $t < 0$, fast oscillations appear for $t > 0$ which break the symmetry (2.4). They are clearly visible for $\epsilon = 0.15$ and $\epsilon = 0.125$; for $\epsilon = 0.1$ they are too weak to be distinguished directly but would appear in the difference between y and some sufficiently good balanced approximation y_{bal} . Note that an integration time much longer than that shown in Figure 1 would reveal a succession of transient events similar to the one occurring near $t = 0$, with, correspondingly, a succession of changes in the amplitude of the fast oscillations. This large-time behaviour, mentioned in the Introduction,

is however not the concern of this paper. Thus, implicit to our discussions, will be the assumption that t is small enough for the single transient event near $t = 0$ to be relevant. Assuming $\epsilon t \ll 1$ is certainly sufficient.

Our objective is to provide an analytic estimate for the amplitude of the fast inertia-gravity oscillations. To separate them from the balanced component of the dynamics, we write

$$x = x_{\text{bal}} + x_{\text{igw}} \quad \text{and} \quad y = y_{\text{bal}} + y_{\text{igw}}, \quad (2.5)$$

with similar expressions for u , v and w . Here, the balanced approximations x_{bal} and y_{bal} are taken to some finite truncation order N , ideally the optimal truncation order (where the series (2.3) reach their least term). For the homoclinic solution (2.2) and for large $|t|$, the choice of N is not crucial and $N = 0$ can be taken because the rapid decay of u_0 and w_0 with $|t|$ leads to terms $x_n, y_n, \dots, n \geq 1$ which are very small except for n exceedingly large. For moderate values of $|t|$ the choice of N is more delicate; a practical approach to find a near-optimal N is discussed in §4.

We remark that it is not a priori obvious whether the separation (2.5) between balanced and inertia-gravity-wave components is a useful one. A difficulty is that x_{bal} and y_{bal} are effectively defined up to exponentially small (slow) terms, depending on the precise value taken for N (at an $O(1)$ distance from its optimal value). These terms could be of the same order as or larger than the rapidly oscillating terms which one wants to associate with x_{igw} and y_{igw} . However, Berry's analysis of the Stokes phenomenon (Berry 1989) suggests that they are in fact asymptotically smaller, so x_{igw} and y_{igw} genuinely represent the rapidly oscillating inertia-gravity waves. This justifies the separation (2.5) and explains why similar approaches have been used successfully (Warn & Menard 1986, Bokhove & Shepherd 1996).

At leading order, the inertia-gravity-wave components x_{igw} and y_{igw} are given by

the homogeneous solution of (2.1)

$$x_{\text{igw}} \sim C \cos(t/\epsilon + \phi) \quad \text{and} \quad y_{\text{igw}} \sim C \sin(t/\epsilon + \phi) \quad (2.6)$$

for some real C and ϕ . (The inertia-gravity-wave component of u , v and w is a factor ϵ^2 smaller (see (2.1)) and will not be considered further.) We examine solutions which are well balanced, i.e. which have $C = 0$ at some initial time $t < 0$. It can be shown that C remains 0 (and ϕ a constant) until t reaches a small neighbourhood of $t = 0$ where a Stokes phenomenon (Olver 1974, Ablowitz & Fokas 1997) takes place. There, exponentially small fast oscillations are switched on: C jumps to a non zero, exponentially small value, and ϕ changes. The oscillations then persist with the same amplitude C and phase ϕ for an asymptotically long (but finite) time.

In the next section, we use exponential asymptotics to estimate the amplitude C analytically. (The reader not interested in the derivation of C may directly skip to equation (3.8) which gives the final result.) Numerical experiments are used in §4 to confirm this estimate and to describe the behaviour of the inertia-gravity oscillations in the switching-on region around $t = 0$.

3 Exponential asymptotics

The divergence of the balanced series (2.3) and the generation of exponentially small oscillations can be traced to the singularities of the terms of (2.3) in the complex t -plane and to the Stokes lines which emanate from these singularities and across which exponentially small terms can be switched on. The leading-order terms (2.2) and higher-order terms indicate that the singularities of (2.3) are located at $t = i(\pi/2 + k\pi)$, $k \in \mathbb{Z}$. The ones closest to the real axis, i.e. $t = \pm i\pi/2$, dominate the asymptotics; here we consider the contribution of the singularity at $t = t_\star = i\pi/2$, given that the contribution of $t = -i\pi/2$ is simply its complex conjugate.

In general, Stokes lines are curves in the complex t -plane where one asymptotic solution is maximally dominant over another asymptotic solution. Writing the dominant and subdominant controlling behaviour of $x(t)$ (or $y(t)$) as $\exp[\phi_+(t)/\epsilon]$ and $\exp[\phi_-(t)/\epsilon]$, respectively, the Stokes lines emanating from t_* are equivalently defined by the condition

$$\text{Im} [\varphi_+(t) - \varphi_-(t)] = \text{Im} [\varphi_+(t_*) - \varphi_-(t_*)]. \quad (3.1)$$

In our context, the dominant term is the balanced component, with $\varphi_+ = 0$, and the subdominant term is the inertia-gravity-wave component, with $\varphi_- = -it$ (cf. (2.6) and (3.3) below; the solution with $\varphi = it$ would be exponentially large for real t so its amplitude remains zero). Thus, according to (3.1), $\text{Re } t = \text{Re } t_* = 0$ consists of Stokes lines; the relevant Stokes line is in fact the segment joining $-\pi/2$ to $\pi/2$. With t real as should physically be the case, the generation of the exponentially small term associated with inertia-gravity waves occurs therefore at $t = 0$. See Figure 2 for an illustration.

A standard approach to calculate this term relies on the complexification of the time t and on the solution of the differential equations (2.1) in a neighbourhood of the singularity t_* using matched asymptotics. The central idea is that near t_* the dominant and subdominant terms have comparable orders of magnitude so that both can be estimated using standard perturbation techniques. This approach is followed here. We only sketch the derivation and refer the reader to Hakim (1998) for a detailed exposition of the method.

Near t_* , we find the leading-order balanced components as

$$u_0 \sim \frac{-i}{t - t_*}, \quad v_0 \sim \frac{-1}{t - t_*}, \quad w_0 \sim \frac{i}{t - t_*}, \quad x_0 \sim \frac{-ib}{(t - t_*)^2}, \quad y_1 \sim \frac{-2ib}{(t - t_*)^3} \quad (3.2)$$

and the inertia-gravity-wave components as

$$x_{\text{igw}} \sim A^\pm e^{-\pi/(2\epsilon)} e^{i(t-t_*)/\epsilon} + B^\pm e^{\pi/(2\epsilon)} e^{-i(t-t_*)/\epsilon},$$

$$y_{\text{igw}} \sim -iA^\pm e^{-\pi/(2\epsilon)} e^{i(t-t_\star)/\epsilon} + iB^\pm e^{\pi/(2\epsilon)} e^{-i(t-t_\star)/\epsilon}. \quad (3.3)$$

The \pm superscripts refer to $t \gtrless 0$ for real t or, more generally, to the left and right of the Stokes line for complex t . Assuming the absence of inertia-gravity waves for $t < 0$, we take $A^- = B^- = 0$. On the right of the Stokes line, we expect $A^+ = 0$ and B^+ non zero but exponentially small. An estimate for B^+ is obtained by examining (2.1) in an neighbourhood of t_\star .

In this inner region, we use the rescaled time variable τ defined by

$$t = t_\star + \epsilon\tau.$$

The asymptotic behaviours (3.2) suggest the introduction of the rescaled dependent variables

$$U = \epsilon u, \quad V = \epsilon v, \quad W = \epsilon w, \quad X = \epsilon^2 x, \quad Y = \epsilon^2 y.$$

Introducing these rescaled variables into (2.1), we find the inner version of the five-component model,

$$\begin{aligned} U' &= -VW + bVY, \\ V' &= UW - bUY, \\ W' &= -UV, \\ X' &= -Y, \\ Y' &= X + bUV, \end{aligned} \quad (3.4)$$

where $'$ denotes differentiation with respect to τ . Somewhat disappointingly, this inner system is nothing other than the full Lorenz system (2.1) with $\epsilon = 1$, so that a complete analytical solution of inner problem cannot be expected. However, such a complete solution is not needed: what is required for matching with the outer problem is the behaviour of the solution for large $|\tau|$ and, more specifically, a connection

formula relating the form of the solution on either side of the Stokes line $\arg \tau = -\pi/2$ (see Figure 2). Here, we obtain this connection formula using a Borel-summation technique (Hakim 1991, Hakim 1998).

For large $|\tau|$, the solution of (3.4) can be sought in the form of series expansions

$$\begin{aligned} U &= \sum_{n=1}^{\infty} \frac{U_n}{\tau^{2n-1}}, & V &= \sum_{n=1}^{\infty} \frac{V_n}{\tau^{2n-1}}, & W &= \sum_{n=1}^{\infty} \frac{W_n}{\tau^{2n-1}}, \\ X &= \sum_{n=1}^{\infty} \frac{X_n}{\tau^{2n}}, & Y &= \sum_{n=1}^{\infty} \frac{Y_n}{\tau^{2n+1}}. \end{aligned} \quad (3.5)$$

Matching with (3.2) gives the $n = 1$ coefficients as

$$U_1 = -i, \quad V_1 = -1, \quad W_1 = i, \quad X_1 = -ib, \quad Y_1 = -2ib.$$

The higher-order coefficients are then derived easily from the recurrence relations that obtain when the series expansions (3.5) are introduced into (3.4). These coefficients are growing rapidly with n suggesting that the series are asymptotic and not convergent.

The required connection formula depends on the form of the (late) coefficients X_n and Y_n for $n \gg 1$. An examination of the recurrence relations indicates that these coefficients have the form

$$X_n \sim i(-1)^n(2n-1)! \kappa \quad \text{and} \quad Y_n \sim i(-1)^n(2n)! \kappa, \quad (3.6)$$

where κ is a function of b that can be estimated numerically (see below). The connection formula is then found using Borel summation. Concentrating on Y for convenience, we define its Borel transform $B_Y(\xi)$ as the series

$$B_Y(\xi) = \sum_{n=1}^{\infty} \frac{Y_n}{(2n)!} \xi^n$$

which is clearly convergent for $|\xi| < 1$. A straightforward calculation then shows that the series for Y is recovered formally from the inversion formula

$$Y(\tau) = \frac{1}{\tau} \int_0^{\infty} e^{-s} B_Y(s^2/\tau^2) ds. \quad (3.7)$$

In this form, Y is a solution of (3.4) which can be made analytic by a suitable choice of integration path; this makes it possible to connect the solution analytically across the Stokes line $\arg \tau = -\pi/2$.

We note from the late coefficients $Y_n/(2n)! \sim i(-1)^n \kappa$ in the expansion of $B_Y(\xi)$ in powers of ξ that $B_Y(\xi)$ is singular for $\xi = -1$, with the behaviour

$$B_Y(\xi) \sim \frac{i\kappa}{1+\xi}.$$

Correspondingly, the integrand in (3.7) has poles for $s = \pm i\tau$. These poles move as t travels along the real axis: in particular, we note that $-\pi < \arg \tau < -\pi/2$ for $t < 0$, and $-\pi/2 < \arg \tau < 0$ for $t > 0$ (see Figure 2). If we take the integration path in (3.7) to be along the positive real axis when $-\pi < \arg \tau < -\pi/2$, then the singularities do not contribute to $Y(\tau)$. This solution matches the oscillation-free $y_{\text{bal}}(t)$ for $t < 0$. As $\arg \tau$ increases beyond $-\pi/2$, the pole $s = i\tau$ crosses the positive real axis and the integration path in (3.7) must be deformed for $Y(\tau)$ to be analytic (see Figure 3): thus, for $-\pi/2 < \arg \tau < 0$, the integral in (3.7) includes the contribution of the pole $s = i\tau$. It is this contribution, readily calculated to be

$$Y_{\text{igw}}(\tau) = -i\pi\kappa e^{-i\tau},$$

which matches the oscillatory term $y_{\text{igw}}(t)$ for $t > 0$. Matching with (3.3) gives $A^+ = 0$ and

$$B^+ = -\pi\kappa\epsilon^{-2}e^{-\pi/(2\epsilon)}.$$

Taking into account the contribution of the singularity at $t = -t_*$, complex conjugate that to just obtained, we find that the inertia-gravity-wave amplitude in (2.6) is

$$C = 2\pi\kappa\epsilon^{-2}e^{-\pi/(2\epsilon)} \tag{3.8}$$

while the phase is $\phi = \pi$. Note that the small parameter ϵ is present in the prefactor besides appearing in the exponential as expected. The ϵ^{-2} -dependence of the prefactor

takes its proper meaning when one recalls that, with the scaling chosen, the balanced component of the fast variable x is $O(1)$ (see (2.2)).

The central formula (3.8) becomes practically useful once the dependence of the prefactor κ on b is established. This dependence is found numerically from (3.6), written as

$$\kappa = \lim_{n \rightarrow \infty} \kappa_n, \quad \text{where} \quad \kappa_n = \frac{i(-1)^{n+1} Y_n}{(2n)!},$$

and where the Y_n are calculated using the recurrence relations for the coefficients in the inner expansion (3.5). The estimates κ_n thus obtained turn out to converge quite slowly with n when b is not small; to accelerate convergence, we have employed a form of second-order Richardson extrapolation based on the assumption that $\kappa_n = \kappa + a_1/n + a_2/n^2 + \dots$ for given constants a_1 and a_2 (Byatt-Smith 2000). With this method, converging results with a relative accuracy of 10^{-4} are obtained in a reasonable number of iterations.

The estimate of κ for a few values of b as well as the number of iterations required are reported in Table 1. A more complete picture is given by Figure 4 which displays κ as a function of b for $0 \leq b \leq 6$. (As many as 78 iterations were required to estimate κ with the desired accuracy when $b = 6$.) Interestingly, the curve, while increasing for small b , is non-monotonic and appears to decay to zero for large b . This implies that the spontaneous generation of inertia-gravity waves can in fact be decreased by increasing the rotational Froude number b . (The maximum of κ can be located accurately as $\kappa = 0.4660$ for $b = 0.7444$.) Also, κ vanishes for several values of b ; for these values, the inertia-gravity-wave generation associated with the singularities of the balanced motion at $t = \pm i\pi/2$ vanishes at leading order. This does not necessarily imply that the wave generation vanishes exactly for values of b close to those for which $\kappa = 0$: the contribution of lower-order terms in the perturbation expansion, and the role of the singularities at $t = i(\pi/2 + k\pi)$, $k \in \mathbb{Z} \setminus \{-1, 0\}$ need

to be considered before definite conclusions are drawn.

Lorenz & Krishnamurthy (1987) derived an estimate for the inertia-gravity-wave amplitude in the limit of small b (see also Camassa (1995) and Camassa & Tin (1996) for studies of the small- b regime). In our notation, this estimate reads

$$C_{\text{LK}} = 2\pi b \epsilon^{-2} e^{-\pi/(2\epsilon)}, \quad (3.9)$$

corresponding to (3.8) with b replacing κ . It follows readily from (2.1) when the first two equations are simplified by discarding the terms proportional to b so that the evolution of (u, v, w) decouples from that of (x, y) . A priori the estimate (3.9) assumes that $b \ll \epsilon$ because it is obtained by taking $b \rightarrow 0$ before $\epsilon \rightarrow 0$. However, our approach recovers it as a limiting case. Indeed, it can be shown that

$$\kappa \sim b \quad \text{for } b \ll 1, \quad (3.10)$$

i.e. (3.8) reduces to (3.9) for small b . The limited range of validity of the linear approximation (3.9)–(3.10) appears in Figure 4 which shows this approximation to κ as well as the exact value. In particular, for the realistic choice $b = 0.5$ made by Lorenz & Krishnamurthy (1987), (3.9) overestimates the actual value $\kappa = 0.4077$ by about 20%.

4 Comparison with numerical results

In this section, we employ numerical solutions of (2.1) to verify the analytic result (3.8) and to examine the generation of inertia-gravity waves for $t \approx 0$. For this we need to extract the inertia-gravity-wave components $x_{\text{igw}}(t)$ and $y_{\text{igw}}(t)$ from the numerical solutions for $x(t)$ and $y(t)$. As mentioned in §2, this can in principle be achieved by subtracting from $x(t)$ and $y(t)$ a balanced approximation $x_{\text{bal}}(t)$ and $y_{\text{bal}}(t)$. There are, however, difficulties with the direct use of such balanced approximations. As

pointed out by Warn et al. (1995), secular terms appear in the evolution equations, which invalidate the approximations for large times. These difficulties are overcome either by using multiple time scales or by using slaving. The slaving approach provides a balanced approximation by regarding the fast variables (x, y) as functions of the slow ones (u, v, w) (Warn et al. 1995). Introduction of such a slaving relation into (2.1) then leads to the so-called superbalance equation (Lorenz 1980) which can be solved asymptotically, order-by-order in ϵ . We use this approach.

Specifically, neglecting terms of order $O(\epsilon^{2N+2})$ for some fixed N , we write the slaving relations as

$$x_{\text{sla}}^N(u, v, w) = \sum_{n=0}^N \epsilon^{2n} \hat{x}_n(u, v, w) \quad \text{and} \quad y_{\text{sla}}^N(u, v, w) = \sum_{n=0}^N \epsilon^{2n+1} \hat{y}_n(u, v, w)$$

and derive the functions \hat{x}_n and \hat{y}_n by introduction into (2.1). The first few are given by

$$\hat{x}_0 = -buv, \quad \hat{y}_0 = b(u^2 - v^2)w, \quad \hat{x}_1 = b(uv^3 - u^3v - 4uvw^2), \dots$$

and can be verified against those obtained by Bokhove & Shepherd (1996) who used the reduction of (2.1) to a two-degree-of-freedom Hamiltonian system. Higher-order terms are derived using a symbolic computation package for N up to 7, i.e. for a first neglected term of order $O(\epsilon^{16})$.

With the slaving relations, a balanced approximation $(u_{\text{bal}}, v_{\text{bal}}, w_{\text{bal}})$ to (u, v, w) is obtained by solving numerically the corresponding balanced model which consists of the first three equations of (2.1) where $x_{\text{sla}}^N(u, v, w)$ and $y_{\text{sla}}^N(u, v, w)$ are substituted for x and y . The inertia-gravity-wave component of x could then be calculated as the difference $x_{\text{igw}} = x - x_{\text{sla}}(u_{\text{bal}}, v_{\text{bal}}, w_{\text{bal}})$, and similarly for y . However, we found it expedient to avoid the integration of the balanced model, using the approximations

$$x_{\text{igw}} \approx x - x_{\text{sla}}(u, v, w) \quad \text{and} \quad y_{\text{igw}} \approx y - y_{\text{sla}}(u, v, w),$$

where (u, v, w) come from the full numerical solutions, i.e. include fast inertia-gravity oscillations. This approximation is a valid one because the inertia-gravity-wave part of (u, v, w) is, as (2.1) indicates, smaller than that of (x, y) by a factor ϵ^2 .

As a measure of the amplitude of the inertia-gravity waves we therefore introduce

$$I^N = \left\{ [x - x_{\text{sla}}^N(u, v, w)]^2 + [y - y_{\text{sla}}^N(u, v, w)]^2 \right\}^{1/2}.$$

The numerical evaluation of I^N provides the desired estimate for the amplitude C : starting with the leading-order balanced solution (2.2) at some large negative t (or more generally with a near-optimal balanced solution for any negative t outside a neighbourhood of 0), we find that $I^N = 0$ for $t < 0$. After a sharp transition near $t = 0$ which we describe below, I^N tends to a constant value,

$$I^N(t) \rightarrow C_{\text{num}} = C[1 + O(\epsilon)], \quad (4.1)$$

essentially independent of N for $t > 0$. Computations for several values of b and ϵ confirm this is the case and provide a verification for the theoretical expression (3.8) for C . Figure 5 shows typical results: it compares the theoretical C with its numerical estimate C_{num} as a function of ϵ for $b = 0.5$ and for $b = 1.5$. The agreement is excellent, particularly for $b = 0.5$, and the discrepancies, decreasing with ϵ , are consistent with the linear error in (4.1).

Figure 6 refines the comparison between theoretical and numerical estimates of the inertia-gravity-wave amplitude by showing the factor κ in (3.8) as a function of b . The theoretical value is compared with two numerical approximations $C_{\text{num}}\epsilon^2 \exp[\pi/(2\epsilon)]/(2\pi)$ obtained for $\epsilon = 0.08$ and 0.06 . The agreement is good for small b but degrades as b increases, suggesting that the error term in (4.1) is rapidly increasing with b . This is supported by a third estimate, obtained from the two numerical approximations by linear extrapolation, which gives a significantly improved agreement with the theoretical κ for b as large as 2. This third estimate is reported as κ_{num} in Table 1.

The recognition that the inertia-gravity-wave generation is associated with a Stokes phenomenon makes it possible not only to estimate the final amplitude of the waves but also to describe the details of the wave growth in the neighbourhood of $t = 0$. Berry (1989) described the smooth manner with which exponentially small terms are switched on across a Stokes line; remarkably, this transition is universal and represented by a simple error function. In our context, his results suggest that the inertia-gravity-amplitude evolves as

$$I^N(t) \approx \frac{C}{2} \left[1 + \operatorname{erf} \left(\frac{t}{(\pi\epsilon)^{1/2}} \right) \right]. \quad (4.2)$$

Here, it is crucial for the approximate equality that N be chosen optimally or near optimally; that is, the series defining x_{sla} and y_{sla} must be truncated near their least term.

Formula (4.2) shows that inertia-gravity waves grow over a time of order $O(\epsilon^{1/2})$. Since t has been non-dimensionalised by the slow (nonlinear) time scale, this means that the transition appears brusque in the slow time, but gentle in the fast time t/ϵ , extending in fact over a large, $O(\epsilon^{-1/2})$, number of inertia-gravity-wave periods.

The behaviour predicted by (4.2) can be verified numerically. Figure 7 shows I^N , scaled by the theoretical amplitude C , as a function of the scaled time $t/(\pi\epsilon)^{1/2}$ for $b = 0.5$, $\epsilon = 0.1$, and for a few values of N . The figure illustrates the importance of a suitable choice of N for the good agreement between the left-hand and right-hand sides of (4.2): as N increases from 4 to 6, the agreement improves; it is of about the same quality for $N = 6$ and $N = 7$ but would degrade for larger N . Figure 7 exemplifies the pragmatic approach we have taken to determine an optimal value for N , choosing it so as to minimise the fluctuations in I^N around the smooth error-function profile. Note, however, how the amplitude for $t/(\pi\epsilon)^{1/2} \gg 1$ is unaffected by the choice of N . This confirms the inconsequence of N for the numerical estimate of C . The discrepancy between this “final” amplitude, i.e. C_{num} , and the theoretical value

C causes the bulk of the mismatch between I^N and the error-function prediction; had I^N been scaled by C_{num} rather than C in Figure 7, a much better agreement would have been obtained.

Figure 8 shows I^N/C as a function of $t/(\pi\epsilon)^{1/2}$ in a manner similar to Figure 7 but for several values of ϵ . For each of these, N has been chosen optimally as explained above. The figure demonstrates the collapse of the evolution of the inertia-gravity-wave amplitude on the universal error-function form when the proper scaling is employed. Again, the agreement between the numerical results and the error-function curve would be improved if the discrepancy between the large- t amplitude C_{num} and its theoretical counterpart C had been accounted for. Note that figures very similar to Figures 7 and 8 can be obtained for a range of values of b ; this confirms that, at leading order in ϵ , the dependence of the inertia-gravity-wave generation on b is only through κ .

It will be noticed that our numerical results are limited to moderately small values of ϵ . This is convenient for two reasons: first, this ensures that the amplitude of the inertia-gravity waves is large enough to dominate any numerical errors; second, the optimal value of N is small enough that the N -term slaving series can be easily calculated. The disadvantage is, of course, that the $O(\epsilon)$ errors involved in the asymptotics are significant. They are sufficiently small, however, for the numerics to provide a convincing verification of the asymptotic results.

5 Concluding remarks

This paper complements that of Lorenz & Krishnamurthy (1987) by providing an analytic estimate for the amplitude of the inertia-gravity waves that are generated spontaneously in the Lorenz (1986) five-component model with $\epsilon \ll 1$ and $b = O(1)$.

The analytic estimate confirms the main conclusion of the mostly numerical analysis of Lorenz & Krishnamurthy (1987): the generation of inertia-gravity waves by balanced motion is inevitable, but it is also very weak, with an amplitude which is exponentially small in ϵ . (A variety of other arguments suggests this exponential scaling; see the Introduction to Vanneste & Yavneh (2003) for a brief review.)

Our estimate reduces to that derived by Lorenz & Krishnamurthy (1987) in the limit of small rotational Froude number $b \ll 1$. In this limit, the slow variables (u, v, w) can be decoupled from the fast ones (x, y) (in effect the terms proportional to b are dropped in the first two equations of (2.1) but retained in the last equation), and (x, y) obey the equations of a forced linear oscillator. In view of the ambiguity of some of the literature (Fowler & Kember 1996), it is worth stressing that the decoupled system is a valid approximation to (2.1) only when $b \ll 1$. For $b = O(1)$, the feedback of (x, y) on (u, v, w) is crucial in determining the amplitude of the inertia-gravity waves. This may not be obvious from (2.1) since the feedback terms are $O(b\epsilon^2) \ll 1$, but it emerges clearly both from our asymptotic analysis (see the inner equations (3.4)) and from the comparison between the exact value of κ and that found for the decoupled system, namely $\kappa \sim b$ (see Figure 4). The sensitivity of the inertia-gravity-wave amplitude to the feedback of the fast variables on the slow variables is related to the exponential smallness of this amplitude; it is a somewhat subtle feature which can be expected to be generic to the generation of inertia-gravity waves in the regime where $R \ll 1$ and $b = O(1)$.

A novel aspect of spontaneous wave generation in the Lorenz–Krishnamurthy model appears in this paper, namely the description of the growth of the waves as t crosses a Stokes line. Several points can be made: (i) the details of the growth can be captured accurately by subtracting from the fast variables their slaving approximation provided that this be near-optimally truncated; (ii) the near-optimal

truncation, when used for initialisation, leads to variables which are practically free of inertia-gravity waves (more precisely, the initial amplitude of inertia-gravity waves is negligible compared to that amplitude attained as a result of spontaneous generation); (iii) the inertia-gravity-wave growth takes place over a short (slow) time scale of order $O(\epsilon^{1/2})$ and is described by an error function; and (iv) because the time scale is so short, dissipative processes, neglected here and very weak in reality, are unimportant for the amplitude of the waves immediately after generation.

It is tempting to transpose these conclusions directly to the problem of wave generation in the real atmosphere and oceans. However, it should be kept in mind that they have been obtained for a severely truncated and highly simplified model. The atmosphere and oceans are accurately described by partial-differential equations rather than the ordinary differential equations considered here, and this may introduce significant physical differences in addition to (considerable) technical difficulties.¹ Furthermore, even in the context of low-order models, the Lorenz–Krishnamurthy model suffers important limitations.

One of these is the absence of certain forms of coupling between the fast and slow variables. In particular, products of slow and fast variables are absent from the evolution equations for the fast variables. Such products, which can be interpreted as nonlinear frequency shifts for the fast variables, affect the amplitude of the inertia-gravity waves, possibly even through the exponential factor (here simply $\pi/(2\epsilon)$). This is evident from the work of Vanneste & Yavneh (2003) where the only terms

¹The limitations of low-order models for the wave-generation problem appear clearly in the low-Froude-number regime, with $b \ll 1$ and $R = O(1)$, where the main mechanism is Lighthill radiation (Ford, McIntyre & Norton 2000). Because this mechanism relies on the (resonant) excitation of inertia-gravity waves with asymptotically large scale, it cannot be captured in low-order models with a single typical spatial scale. See Saujani & Shepherd (2002) and Ford, McIntyre & Norton (2002) for a discussion contrasting the low-Froude-number and low-Rossby-number regimes.

leading to inertia-gravity-wave generation are of this type. Clearly, the analysis of a low-order model in which all realistic types of fast-slow interactions are represented would be useful.

Another limitation of the Lorenz–Krishnamurthy model is the integrability of the slow dynamics. This has been considered by Wirosuetisno & Shepherd (2000) who introduced an extension of the model making its slow dynamics chaotic. It would be interesting to apply exponential-asymptotic techniques to this extended model. In general, one might expect chaotic dynamics to lead to a more complex singularity structure of the slow variables for complex t than the presence of a few poles. For instance, if the conjecture on the Painlevé integrability is true (Ercolani & Siggia 1990, and references), chaotic (non-integrable) systems must at least have some branch points; but much more exotic behaviour is certainly possible. Although such behaviour may lead to much technical complications, it is unlikely to alter the essential conclusion that the inertia-gravity waves generated are exponentially small. The only requirement for this to hold is the smoothness of the balanced variables for real values of t , with all singularities some distance away from the real axis. This leads to the balanced variables having an exponentially decaying frequency spectrum and hence an exponentially small amplitude at the $O(1/\epsilon)$ frequency of the fast variables (cf. Warn (1997)).

In the partial-differential-equation context, an exponentially decaying frequency spectrum of the balanced variables is presumably also sufficient to lead to exponentially small inertia-gravity waves. However, one might question whether real balanced flows have such a spectrum. Real flows are turbulent and, according to Kolmogorov-type arguments, often have power-law, not exponential, frequency spectra. This would imply inertia-gravity-wave amplitudes that are algebraic, not exponential, in ϵ . But balanced turbulence is special, and it can be argued that its frequency spectrum

does decay exponentially: if we assume that balanced turbulence behaves more-or-less like quasi-geostrophic turbulence, then its energy spectrum $E(k)$, where k is the wavenumber, is likely to be the power law k^{-3} (in the direct enstrophy cascade) or steeper. Correspondingly, the typical frequency $\omega \propto k[kE(k)]^{1/2}$, or more precisely $\omega \propto (\int k^2 E(k) dk)^{1/2}$, is predicted to be essentially independent of k , i.e. to be fixed by the temporal behaviour of the large-scale motion (Kraichnan 1971).² Because this is presumably smooth, an exponential frequency spectrum $E(\omega)$ can be expected. (This conclusion may be contrasted with that obtained for a different regime of turbulence, say the inverse energy cascade with $E(k) \propto k^{-5/3}$, which gives $\omega \propto k^{2/3}$ and the power-law frequency spectrum $E(\omega) \propto \omega^{-5/2}$.) It would be interesting to confirm (or refute) this heuristic argument using direct numerical simulations.

Acknowledgements. It is a pleasure to thank O. Bokhove J. G. Byatt-Smith, A. Olde Daalhuis and I. Yavneh for discussions and comments. JV is funded by a NERC Advanced Fellowship. Additional support was provided by the EPSRC Network in Mathematics “Geometric Methods in Geophysical Fluid Dynamics”.

A Periodic balanced solutions

For $\epsilon = 0$, the general solution of (2.1) can be written explicitly in terms of Jacobian elliptic functions. Here, we consider the one-parameter family of solutions

$$u_0 = \operatorname{cn}(t/k, k), \quad v_0 = -\operatorname{sn}(t/k, k), \quad w_0 = -\operatorname{dn}(t/k, k)/k, \quad x_0 = -bu_0v_0, \quad y_0 = 0, \quad (\text{A.1})$$

²The same reasoning indicates that that balanced approximations remain self-consistent, without breakdown at small scales, because the Rossby number ω/f is independent of k (Warn & Menard 1986).

parameterised by $0 < k \leq 1$, which reduce to the homoclinic solution (2.2) for $k = 1$. The solutions (A.1) are periodic, with fourth-period $kK(k)$, where $K(k)$ is the complete elliptic integral of the first kind. They also have poles on a lattice in the complex t -plane. (The solutions (A.1) are in fact very general: using the symmetries of (2.1), one can impose $u_0(0) = 1$ $v_0(0) = 0$ by suitable definitions of ϵ and of the origin for t , leaving the condition $|u_0(0)/w_0(0)| = k \leq 1$ as the only restriction; when the opposite condition holds, the roles of u_0 and w_0 have to be interchanged.)

We are interested in the inertia-gravity waves that are generated for $\epsilon \neq 0$ from a solution given at leading order by (A.1) that is well balanced at some initial time. To concentrate on a single wave-generation event, i.e. the crossing of a single Stokes line, we take this initial time to satisfy $-kK(k) < t < 0$ and we estimate the wave amplitude at a later time $0 < t < kK(k)$; the waves are then entirely generated at $t = 0$, across the Stokes line $\text{Re } t = 0$ which joins the complex-conjugate poles at

$$t = \pm t_\star = \pm ikK'(k), \quad \text{where } K'(k) = K(\sqrt{1 - k^2}).$$

The exponential-asymptotic calculation yielding the amplitude of the inertia-gravity waves is essentially identical to that carried out in §3 for the homoclinic solution. The sole difference is the different location of the poles, leading to a different exponential behaviour of the amplitude. The determination of the prefactor is, in fact, completely identical, because the leading-order behaviour of the solution in the neighbourhood of the singularities $\pm t_\star$ is independent of k ; in particular, it is the one deduced in §3 for the homoclinic solution. The amplitude of the inertia-gravity waves is therefore found to be

$$C = 2\pi\kappa\epsilon^{-2}e^{-kK'(k)/\epsilon}. \tag{A.2}$$

Note that the function $kK'(k)$ is monotonically increasing from 0 at $k = 0$ to $\pi/2$ at $k = 1$: the generation of inertia-gravity waves is thus minimised for the homoclinic

solution.

We have verified the result (A.2) numerically. When k is significantly less than 1, so that the period of the balanced solution is not particularly large, the numerical estimation of C for small but finite ϵ is somewhat delicate: because the $O(\epsilon^{1/2})$ time interval during which the switching-on of the waves takes place occupies a significant fraction of the period, the use of an accurate slaving solution both for the initialisation and for the estimation of the wave amplitude is essential. In spite of this difficulty, we have obtained good agreement between the theoretical and numerical results. This is illustrated in Figure 9 which shows C (in logarithmic coordinate) as a function of $1/\epsilon$ for two different solutions in the family (A.1). For the first, $k = 2/3$, the period $kK(k)$ is 1.206 and the exponential factor $kK'(k)$ is 1.269; for the second $k = 1/2$, the period is 0.843 and the exponential factor is 1.078.

References

- Ablowitz, M. J. & Fokas, A. S. 1997, *Complex variables: introduction and applications*, Cambridge University Press.
- Berry, M. V. 1989, Uniform asymptotic smoothing of Stokes's discontinuities, *Proc. R. Soc. Lond. A* **422**, 7–21.
- Bokhove, O. & Shepherd, T. G. 1996, On Hamiltonian balanced dynamics and the slowest invariant manifold, *J. Atmos. Sci.* **53**, 276–297.
- Boyd, J. P. 1994, The slow manifold of a five-mode model, *J. Atmos. Sci.* **51**, 1057–1064.
- Boyd, J. P. 1995, Eight definitions of the slow manifold: seiches, pseudoseiches, and exponential smallness, *Dyn. Atmos. Oceans* **22**, 49–75.

- Byatt-Smith, J. G. 2000, The Borel transform and its use in the summation of asymptotic expansions, *Stud. Appl. Math.* **105**, 83–113.
- Camassa, R. 1995, On the geometry of an atmospheric slow manifold, *Physica D* **84**, 357–397.
- Camassa, R. & Tin, S.-K. 1996, The global geometry of the slow manifold in the Lorenz–Krishnamurthy model, *J. Atmos. Sci.* **53**, 3251–3264.
- Ercolani, N. & Siggia, E. D. 1990, Painlevé property and integrability, *in* V. E. Zakharov, ed., *What is integrability?*, Springer–Verlag, pp. 63–72.
- Ford, R., McIntyre, M. E. & Norton, W. A. 2000, Balance and the slow quasi-manifold: some explicit results, *J. Atmos. Sci.* **57**, 1236–1254.
- Ford, R., McIntyre, M. E. & Norton, W. A. 2002, Reply to comments by S. Saujani and T. G. Shepherd on “Balance and the slow quasi-manifold: some explicit results”, *J. Atmos. Sci.* **59**, 2878–2882.
- Fowler, A. C. & Kember, G. 1996, The Lorenz–Krishnamurthy slow manifold, *J. Atmos. Sci.* **53**, 1433–1437.
- Hakim, V. 1991, Computation of transcendental effects in growth problems: linear solvability conditions and nonlinear methods – the example of the geometric model, *in* H. Segur, S. Tanveer & H. Levine, eds, *Asymptotics beyond all orders*, Plenum press, pp. 15–28.
- Hakim, V. 1998, Asymptotic techniques in nonlinear problems: some illustrative examples, *in* C. Godrèche & P. Manneville, eds, *Hydrodynamics and nonlinear instabilities*, Cambridge University Press, chapter 3, pp. 295–386.

- Jacobs, S. J. 1991, Existence of a slow manifold in a model system of equations, *J. Atmos. Sci.* **48**, 893–901.
- Kraichnan, R. H. 1971, Inertial-range transfer in two- and three-dimensional turbulence, *J. Fluid Mech.* **47**, 525–535.
- Lorenz, E. N. 1980, Attractor sets and quasi-geostrophic equilibrium, *J. Atmos. Sci.* **37**, 1685–1699.
- Lorenz, E. N. 1986, On the existence of a slow manifold, *J. Atmos. Sci.* **43**, 1547–1557.
- Lorenz, E. N. 1992, The slow manifold — What is it?, *J. Atmos. Sci.* **49**, 2449–2451.
- Lorenz, E. N. & Krishnamurthy, V. 1987, On the nonexistence of a slow manifold, *J. Atmos. Sci.* **44**, 2940–2950.
- Olver, F. W. J. 1974, *Asymptotics and special functions*, Academic Press, New York.
Computer Science and Applied Mathematics.
- Pedlosky, J. 1987, *Geophysical fluid dynamics*, Springer–Verlag.
- Saujani, S. & Shepherd, T. G. 2002, Comments on “Balance and the slow quasi-manifold: some explicit results”, *J. Atmos. Sci.* **59**, 2874–2877.
- Segur, H., Tanveer, S. & Levine, H., eds 1991, *Asymptotics beyond all orders*, Plenum Press, New York.
- Vanneste, J. & Yavneh, I. 2003, Exponentially small inertia-gravity waves and the breakdown of quasi-geostrophic balance, *J. Atmos. Sci.* In press.
- Warn, T. 1997, Nonlinear balance and quasi-geostrophic sets, *Atmos.-Ocean* **35**, 135–145.

Warn, T. & Menard, R. 1986, Nonlinear balance and gravity-inertial wave saturation in a simple atmospheric model, *Tellus* **38A**, 285–294.

Warn, T., Bokhove, O., Shepherd, T. G. & Vallis, G. K. 1995, Rossby number expansions, slaving principles, and balance dynamics, *Quart. J. R. Met. Soc.* **121**, 723–739.

Wirosoetisno, D. & Shepherd, T. G. 2000, Averaging, slaving and balance dynamics in a simple atmospheric model, *Physica D* **141**, 37–53.

List of Figures

1	Fast variable y as a function of time for $b = 0.5$ and $\epsilon = 0.15$ (upper curve, offset by 0.02), $\epsilon = 0.125$ (middle curve, offset by 0.01), and $\epsilon = 0.1$ (lower curve).	1
2	Complex t -plane showing the location of the singularities $\pm i\pi/2$ of the balanced motion and the Stokes line $\text{Re } t = 0$ joining them. The rescaled time variable τ and its argument $\arg \tau$ for a real, negative value of t are also indicated.	2
3	Integration in the complex s -plane of the inversion formula (3.7). For $t < 0$ (left panel), the poles at $\pm i\tau$ do not contribute to the integral; for $t > 0$ (right panel) the integration contour encloses the pole at $i\tau$ which yields an oscillatory contribution.	3
4	Factor κ in (3.8) as a function of the rotational Froude number b (solid line). The dotted line indicates the linear approximation $\kappa \sim b$ valid for $b \ll 1$	4
5	Amplitude of the inertia-gravity waves (in logarithmic coordinate) as a function of $1/\epsilon$ for $b = 0.5$ (+, upper curve) and $b = 1.5$ (\times , lower curve). Numerical results (symbols) are compared with the analytical predictions (curves).	5
6	Numerical estimates for κ as a function of b : estimates obtained for $\epsilon = 0.08$ (+), $\epsilon = 0.06$ (\times) and using a linear extrapolation (\circ) are compared with the theoretical value.	6
7	Scaled inertia-gravity-wave amplitude I^N/C as a function of $t/(\pi\epsilon)^{1/2}$ obtained numerically for $\epsilon = 0.1$ and $b = 0.5$ and for $N = 4, 5, 6, 7$ (solid lines). Also shown is the function $[1 + \text{erf}(t/(\pi\epsilon)^{1/2})]/2$ expected in the limit $\epsilon \rightarrow 0$ for an optimal N (dotted line).	7
8	Scaled inertia-gravity-wave amplitude I^N/C obtained numerically for $b = 0.5$ and for different ϵ , with N chosen optimally (solid lines). The values of $\epsilon(N)$ are 0.1(6), 0.125(5), 0.15(4), 0.175(3) and 0.2(3). (The curves can be identified by their value for large t which increases with ϵ .) The function $[1 + \text{erf}(t/(\pi\epsilon)^{1/2})]/2$ is also shown (dotted line).	8
9	Amplitude of the inertia-gravity waves (in logarithmic coordinate) as a function of $1/\epsilon$ for periodic balanced solutions with $b = 0.5$. Numerical results for $k = 2/3$ (+) and $k = 1/2$ (\times) are compared with the analytical prediction (curves).	9

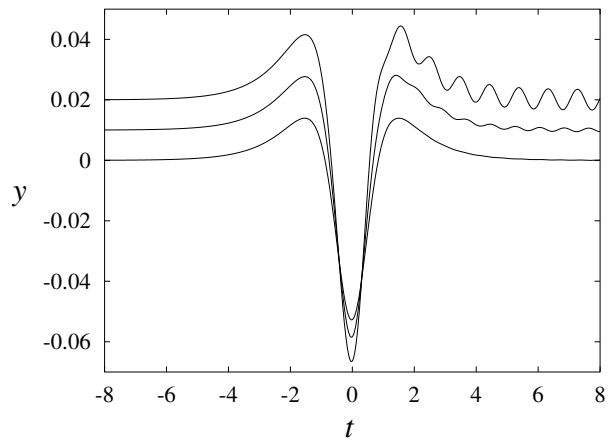


Figure 1: Fast variable y as a function of time for $b = 0.5$ and $\epsilon = 0.15$ (upper curve, offset by 0.02), $\epsilon = 0.125$ (middle curve, offset by 0.01), and $\epsilon = 0.1$ (lower curve).

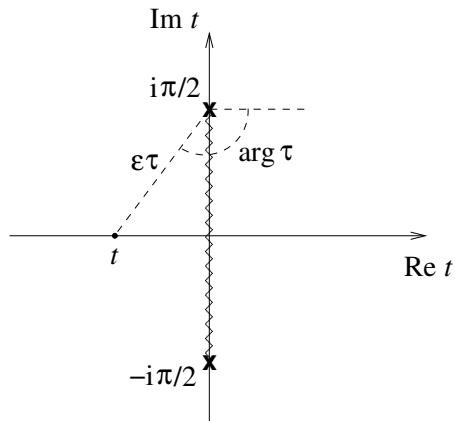


Figure 2: Complex t -plane showing the location of the singularities $\pm i\pi/2$ of the balanced motion and the Stokes line $\text{Re } t = 0$ joining them. The rescaled time variable τ and its argument $\arg \tau$ for a real, negative value of t are also indicated.

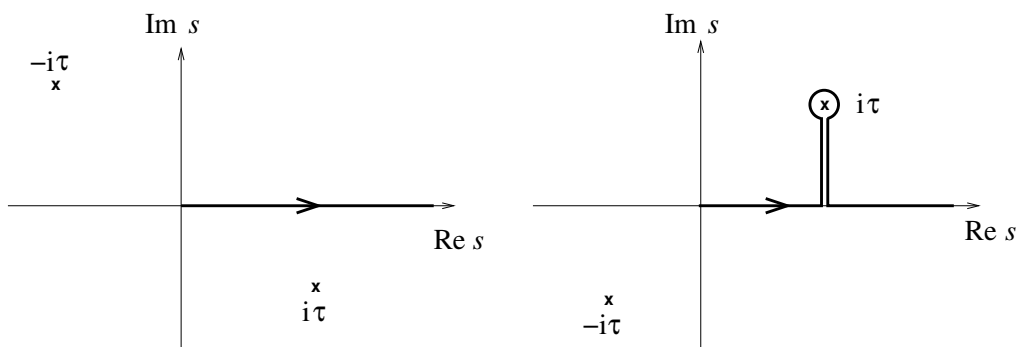


Figure 3: Integration in the complex s -plane of the inversion formula (3.7). For $t < 0$ (left panel), the poles at $\pm i\tau$ do not contribute to the integral; for $t > 0$ (right panel) the integration contour encloses the pole at $i\tau$ which yields an oscillatory contribution.

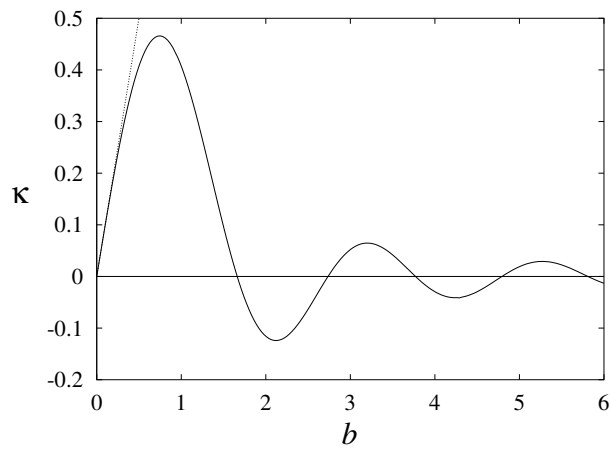


Figure 4: Factor κ in (3.8) as a function of the rotational Froude number b (solid line). The dotted line indicates the linear approximation $\kappa \sim b$ valid for $b \ll 1$.

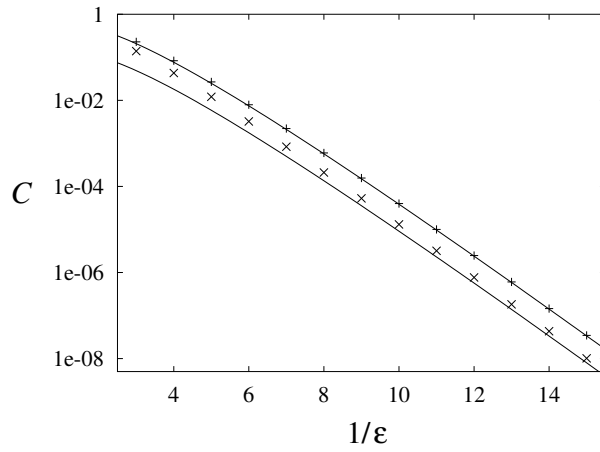


Figure 5: Amplitude of the inertia-gravity waves (in logarithmic coordinate) as a function of $1/\epsilon$ for $b = 0.5$ (+, upper curve) and $b = 1.5$ (\times , lower curve). Numerical results (symbols) are compared with the analytical predictions (curves).

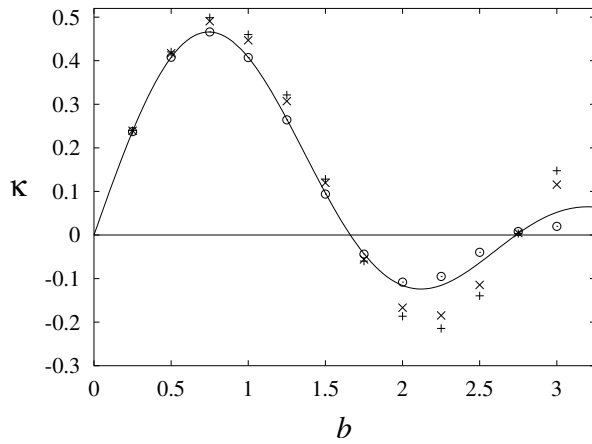


Figure 6: Numerical estimates for κ as a function of b : estimates obtained for $\epsilon = 0.08$ (+), $\epsilon = 0.06$ (\times) and using a linear extrapolation (\circ) are compared with the theoretical value.

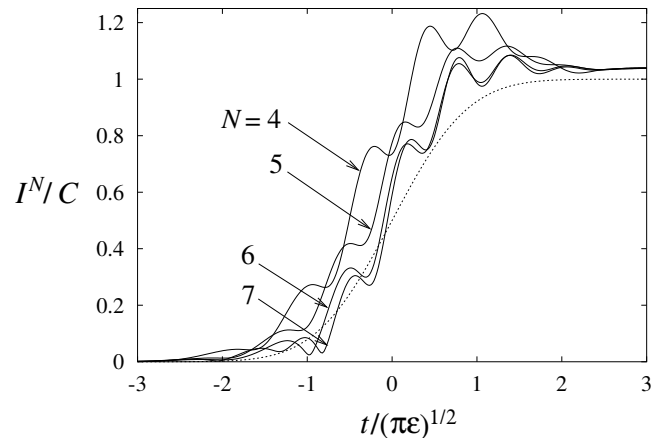


Figure 7: Scaled inertia-gravity-wave amplitude I^N/C as a function of $t/(\pi\epsilon)^{1/2}$ obtained numerically for $\epsilon = 0.1$ and $b = 0.5$ and for $N = 4, 5, 6, 7$ (solid lines). Also shown is the function $[1 + \text{erf}(t/(\pi\epsilon)^{1/2})]/2$ expected in the limit $\epsilon \rightarrow 0$ for an optimal N (dotted line).

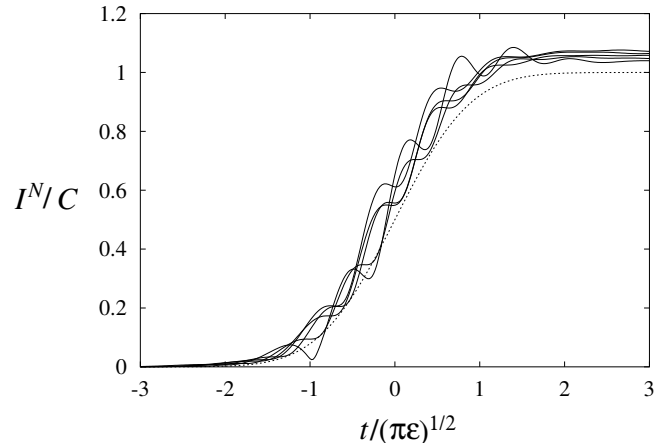


Figure 8: Scaled inertia-gravity-wave amplitude I^N/C obtained numerically for $b = 0.5$ and for different ϵ , with N chosen optimally (solid lines). The values of ϵ (N) are $0.1(6)$, $0.125(5)$, $0.15(4)$, $0.175(3)$ and $0.2(3)$. (The curves can be identified by their value for large t which increases with ϵ .) The function $[1 + \text{erf}(t/(\pi\epsilon)^{1/2})]/2$ is also shown (dotted line).

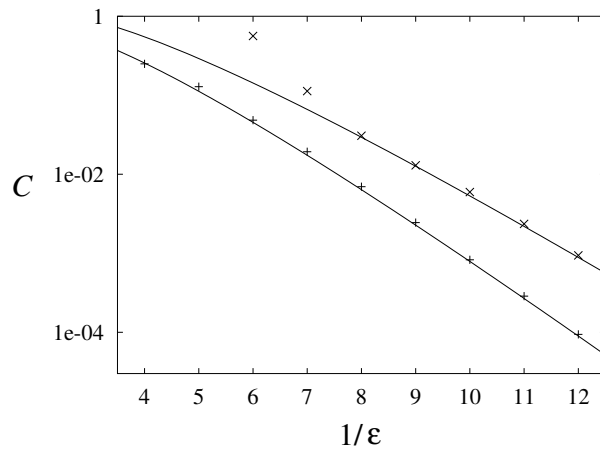


Figure 9: Amplitude of the inertia-gravity waves (in logarithmic coordinate) as a function of $1/\epsilon$ for periodic balanced solutions with $b = 0.5$. Numerical results for $k = 2/3$ (+) and $k = 1/2$ (\times) are compared with the analytical prediction (curves).

List of Tables

1	Values of the factor κ in (3.8) as a function of the rotational Froude number b . Also indicated are the number n of iterations required for the estimation of κ with a relative error of 10^{-4} and an indirect numerical estimate of κ described in §4.	11
---	---	----

b	κ	n	κ_{num}
0.25	0.2378	6	0.2372
0.5	0.4077	6	0.4080
0.75	0.4660	9	0.4660
1.	0.4076	11	0.4073
1.25	0.2657	12	0.2642
1.5	0.0965	13	0.0940
1.75	-0.0430	15	-0.0438
2.	-0.1159	15	-0.1083

Table 1: Values of the factor κ in (3.8) as a function of the rotational Froude number b . Also indicated are the number n of iterations required for the estimation of κ with a relative error of 10^{-4} and an indirect numerical estimate of κ described in §4.